Effects of nonparallel exit flow on round turbulent free jets

W. R. Quinn
Department of Engineering, St. Francis Xavier University, Antigonish, Nova Scotia, Canada B2G 1C0

and J. Militzer
Department of Mechanical Engineering, Technical University of Nova Scotia, Halifax, Nova Scotia, Canada B3J 2X4

Results of an experimental and numerical study of the effects of nonparallel exit flow on round turbulent free jets are presented. Two nozzle types with the same exit area were used: a sharp-edged slot machined into an aluminum plate and a smoothly contoured nozzle manufactured from Plexiglas. Hot-wire anemometry was used to obtain the mean velocity and turbulent normal stress results and the mean static pressure results were acquired with a pitot-static tube and a pressure transducer. An elliptic, finite-volume-based procedure was used in the numerical study which predicted the mean velocity and the mean static pressure. The experimental results show the existence of distinct off-center peaks in the mean streamwise velocity in the very near flow field of the jet from the sharp-edged round slot, which had pronounced nonparallel exit flow. These mean streamwise velocity off-center peaks were absent in the smoothly contoured nozzle jet flow which was found to spread faster than the sharp-edged slot jet flow in the initial region. The agreement between the experimental results and the numerical predictions was found to be excellent for the mean streamwise velocity decay on the jet centerline and the spread of the jet beyond the initial region. Only qualitative agreement can be claimed for the other quantities.

Keywords: round jets; turbulence; sharp-edged orifice; nozzle; mean static pressure

Introduction

The round turbulent jet issuing into virtually unbounded surroundings is useful in a variety of areas of technical interest. This flow configuration has, therefore, been and continues to be the subject of a number of contributions to basic research in fluid mechanics. The flow field can be divided into three regions, namely, an initial or flow development region, a transition region, and a fully developed region.

The fully developed region of the jet has been studied, in detail, experimentally by Wygnanski and Fiedler[1] and by Rodi,[2] among others. Both the mean flow and turbulence structure of the jet exhibit self-similarity in this region of the jet and this has made the analytic treatment of the jet possible. Contributions to the closed-form solutions of the governing partial differential equations for the fully developed region can be found in, for example, Rajaratnam[3] and Schlichting.[4] Finite-difference based numerical studies of the fully developed region have also been done by Rodi,[5] Spalding,[6] Givi and Ramos,[7] and other researchers. The initial and transition regions have also been investigated experimentally and numerically. Some of these investigations, such as those carried out by Davies *et al.*,[8] Bradshaw *et al.*,[9] Ko and Davies,[10] and Lau and Fischer,[11] were in connection with the suppression of jet noise. The studies done by Crow and Champagne[12] and Dimotakis *et al.*[13] were devoted to the understanding of the coherent large-scale structures of the jet. The reader interested in coherent structures is referred to the survey paper by Hussain.[14] Other contributions to the understanding of the initial and transition regions of a round turbulent- free jet have been made by Sami *et al.*,[15] Hill,[16] Boguslawski and Popiel,[17] and Obot *et al.*[18] Reference 15 provides mean flow, mean static pressure and turbulence data for the flow from a smoothly contoured nozzle. Reference 16 documents mass entrainment data for the flow from a short converging round nozzle. Reference 17 presents mean streamwise velocity and turbulence data for the flow that issues, with a fully developed turbulent velocity exit profile, from a long circular pipe. The study reported in Ref. 18 provides mean streamwise velocity data, from which spreading and mass entrainment rates were deduced, for the flow from a square-edged round slot. There is no study, in the extant literature, that examines the flow from a sharp-edged round slot in detail even though this flow configuration occurs in many practical systems. Moreover, only few of the studies mentioned above (e.g., Ref. 18) give sufficient details of the nozzle or slot geometry and of the initial conditions for the results to be interpreted in the proper perspective.

The present study examines, experimentally and numerically, the effects of nonparallel exit flow upon the flow in the initial and transition regions of a round turbulent-free jet. Two nozzle configurations are used: a sharp-edged round slot machined into a plate of aluminum according to BS 1042 and a smoothly contracting round nozzle manufactured from Plexiglas. The radius of curvature of the Plexiglas nozzle is equal to the diameter of the nozzle at the exit plane. Details of both the sharp-edged round slot and the Plexiglas round nozzle are shown in Figure 1. The exit plane Reynolds number, based on the diameter of the slot or nozzle, was about 2.08×10^5. The mean streamwise velocity at the center of the exit plane was

Address reprint requests to Dr. Quinn at the Department of Engineering, St. Francis Xavier University, Antigonish, Nova Scotia, Canada B2G 1C0.

Received 9 May 1988; accepted for publication 18 July 1988

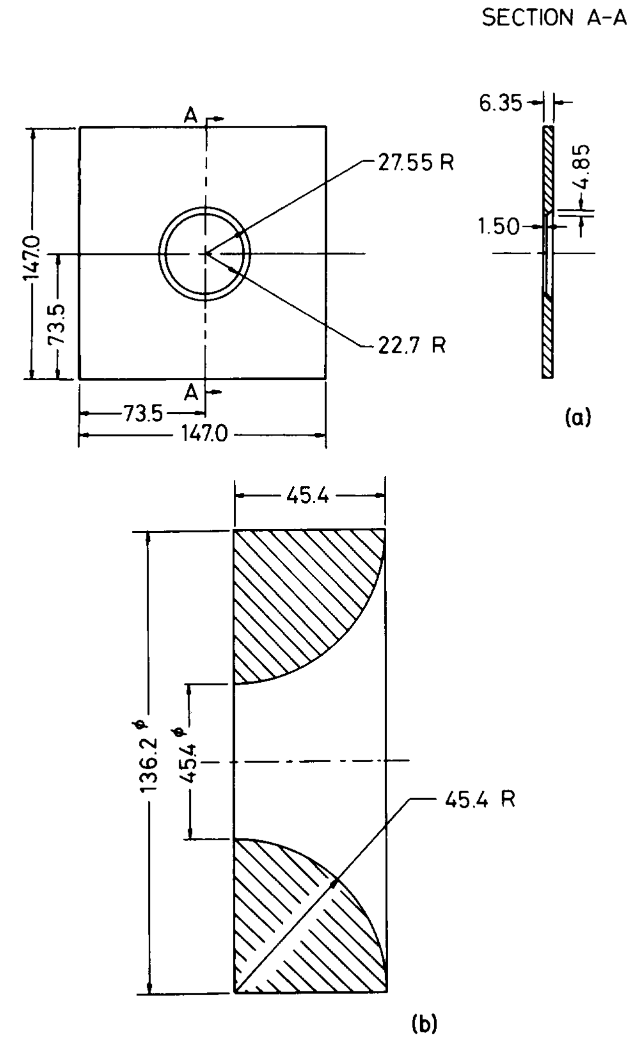

Figure 1 Nozzles: (a) sharp-edged slot; (b) contoured nozzle

60 m/s and the corresponding streamwise turbulence intensity was about 0.5%. The numerical study was done to test the ability of an existing finite-volume-based elliptic code to predict the mean streamwise velocity and the mean static pressure within a round turbulent-free jet in the initial and transition regions. Analytic solutions of the governing partial differential equations are not available for these regions.

Experimental apparatus

A blow-down type of facility, which consists of a centrifugal fan, a settling chamber, a three-dimensional contraction, and the nozzles, was used in the present investigation. The fan, which was mounted on antivibration cork-and-neoprene rubber pads, drew air from a room adjacent to the laboratory and delivered it to the settling chamber. The inlet to the fan was fitted with furnace filters to trap dust particles. The settling chamber, which is a plywood box of 0.76 × 0.76 m cross-sectional area, is 1.23 m long. It has a baffle at the upstream end, aluminum honeycomb with hexagonal cells, which are 0.0032 m in diameter and 0.0508 m long, and five mesh-wire screens of 69% porosity. The three-dimensional contraction, with a cross-sectional area at the inlet of 0.76 × 0.76 m and 0.305 × 0.305 m at the exit, has a contour that is based on a third degree polynomial with zero derivative end conditions. The nozzles, each with an exit plane cross-sectional area of 0.0016 m^2 and 45.4 mm in diameter, were used to cap the exit end of the three-dimensional contraction. This resulted in a contraction ratio of 361. The exit end of the contraction was flush with a 2.44 × 2.44 m plywood wall which was at the upstream end of a screen cage into which the jets issued. The screen cage, extending 3.66 m downstream from the plywood wall, was covered on the top and sides with steel damping screens of 42% porosity. The downstream end of the screen cage was open.

A three-dimensional traversing system, controlled by the 8088 microprocessor of the Commodore PC10-II computer, was employed for moving the sensing probes in the flow field. A rack-and-pinion system was used for traversing in the streamwise (X) direction and lead screws were used for traversing in the spanwise (Y) and lateral (Z) directions. The X and Y coordinate directions lie in a horizontal plane and form a right-hand system with the Z coordinate direction. Traversing was effected by dc stepping motors. Positioning accuracy was 0.3 mm in the X direction and 0.01 mm in the Y and Z directions.

Dantec P11 (single normal) and P61 (x-array) hot-wire probes were used for the mean velocity and turbulence measurements. The hot-wire probes were operated by Dantec 56C01 constant temperature anemometers in conjunction with Dantec 56C17 bridges. Dantec 56N21 linearizers were used to linearize the hot-wire signals. The mean static pressure measurements were made wth a 2.3 mm o.d. pitot-static tube made of stainless steel. The pitot-static tube, with an ellipsoidal head and four static holes as specified by BS 1042 (1973, part A), was connected to a Datametrics pressure transducer and an electronic manometer. The Scientific Solutions labmaster analog-to-digital (A/D) board, which has 12-bit resolution, 16 analog input

Notation

$C_{1\varepsilon}, C_{2\varepsilon}$	Empirical constants
D	Nozzle diameter
k	Turbulence kinetic energy
P	Mean static pressure
$R_{1/2}$	Jet half-width
S_ϕ	Source term
U	Mean streamwise velocity
$\sqrt{\overline{u'^2}}$	Root mean square of fluctuating streamwise velocity
V	Mean radial velocity
$\sqrt{\overline{v'^2}}$	Root mean square of fluctuating spanwise velocity
$\mathbf{v}$	Velocity vector
X	Streamwise Cartesian coordinate
Y	Radial Cartesian coordinate
$Y_{1/2}$	Radial half-width
Γ_ϕ	Diffusion coefficient
ε	Rate of dissipation of turbulence kinetic energy
ϕ	Generalised dependent variable
ρ	Fluid density

Subscripts

atm	Atmospheric value
cl	Centerline value
exit	Value on the centerline at the exit plane

channels, a multiplexer, and a sample-and-hold unit, was used to digitize the hot-wire and mean static pressure signals. Two other sample-and-hold units were used for measurements with the x-array hot-wire probes.

Experimental procedure

The hot-wire probes were calibrated, at a resistance ratio 1.8, in the potential core of the jet at about 0.05 m from the slot exit plane. The mean streamwise velocity distribution was fairly uniform at this location. Calibration of the pitot-static tube confirmed the direct linear relationship between the total and mean static pressure readings in inches of water and the corresponding voltage readings on the electronic manometer.

The mean and rms fluctuating velocities were obtained, depending upon the location in the flow field, by sampling 20,000 to 120,000 points at about 1 kHz. The mean static pressures were obtained by sampling 30,000 points also at about 1 kHz. The data acquisition and some of the data reduction were done on-line and compiled software written in BASIC, using the Turbobasic compiler, was used to speed up the process.

Numerical simulation

The steady-state form of the governing partial differential equations (i.e., for continuity, momentum and turbulence transport) can, according to Patankar,[19] be written in the general form

$$\mathrm{div}(\rho \mathbf{v}\phi - \Gamma_\phi \, \mathrm{grad}\, \phi) = S_\phi \tag{1}$$

The independent variables in this study are X and Y, and the dependent variables are U, V, k, and ε. The mean static pressure P is associated with the continuity equation. Sources and the diffusion coefficients for the dependent variables considered here can be found in Ref. 19. Equation 1 was discretized, using finite differences, following the procedure described in Ref. 19, which also discusses the solution of the resulting algebraic difference equations. Very briefly, the jet flow domain, which was 12 nozzle diameters wide in the Y direction and 35 nozzle diameters long in the X direction, was divided into 3600 control volumes. The centers of the control volumes were at the grid line intersections of a 60×60 grid line nonuniform mesh. The dependent variables, other than the velocities, were calculated at the centers of the control volumes. The velocities were calculated at the centers of the control volume faces. The mean static pressure was computed, at the centers of the control volumes, indirectly from the continuity equation using the SIMPLEST algorithm.[20]

The k-ε turbulence model[21] was used to calculate the Reynolds stresses in the momentum equations. The standard form of the k-ε turbulence model given in Ref. 21 overpredicts, as has been shown by Rodi,[22] the spreading rate of a turbulent free round jet because of the model form of the generation and destruction terms in the ε equation. The model constants $C_{1\varepsilon} = 1.48$ and $C_{2\varepsilon} = 1.90$, with all other model constants having the standard values given in Ref. 21, were found to give reasonable spreading and mean streamwise velocity decay results in the present study.

The flow domain was bounded by an inlet line, an axial symmetry line, a free stream boundary and a downstream boundary. Atmospheric pressure boundary conditions were used at the free-stream and downstream boundaries. The measured mean streamwise and mean radial velocities were used as initial velocity conditions at the inlet line.

The numerical computations were performed with the PHOENICS computer code[23] on the Cyber 170/828 computer. Typical computation time was 0.001 s/control volume/sweep/dependent variable and about 2.5 CPU h were required to obtain a converged solution.

Results and discussion

Flow at the nozzle exit plane

The mean radial velocity profiles at the exit plane of the two nozzles are shown in Figure 2. These mean radial velocities arise, in both flows, from the vena contracta effect. Indeed the mean radial velocities are, as expected, directed inward (i.e., toward the jet centerline) as shown in the figure. The vena contracta effect is more pronounced in the jet from the sharp-edged slot due to the abrupt transiton of the flow from the contraction to the slot exit plane; larger mean radial velocities are, therefore, found in the flow through the sharp-edged slot.

The mean static pressure profiles (Figure 3) and the mean streamwise velocity profiles (Figure 4) at the exit plane are consistent with the fact that the curvature of the streamlines, initiated within the contraction, does not end at the exit plane. Streamline curvature triggers centrifugal acceleration of the fluid particles and a transverse pressure gradient must then be set up to balance the resulting centrifugal forces. Parallel exit flow would prevail in the absence of streamline curvature.

Mean streamwise velocity decay on the jet centerline

The experimental and numerical results for the decay of the mean streamwise velocity along the jet centerline are presented in Figure 5. The vena contracta effect is clearly evident in both flows. The differences in the mean streamwise velocity decay occur in the initial region which is influenced by the nonparallel flow at the exit plane. The acceleration, along the jet centerline, of the jet from the sharp-edged slot is significantly larger than that of the jet from the contoured nozzle. It can be said, based on the evidence at hand, that the acceleration of a fluid particle, on the jet centerline in the initial region, is directly related to the magnitude of the mean radial velocity at the exit plane of the nozzle.

There is excellent agreement between the experimental and numerical results after the initial region. Only qualitative agreement between the experimental and numerical results can be claimed in the initial region. There is one possible reason for this discrepancy, namely, that the grid used for the numerical predictions was probably not fine enough to resolve the large

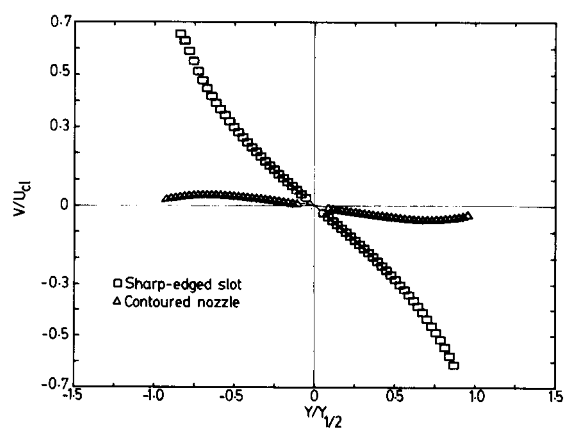

Figure 2 Mean spanwise velocity profiles at the nozzle exit plane

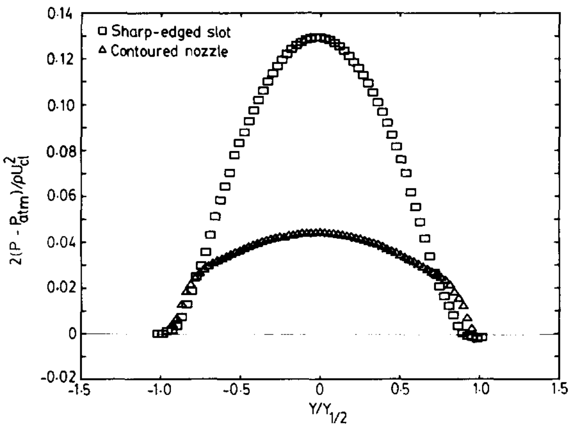

Figure 3 Mean static pressure profiles at the nozzle exit plane

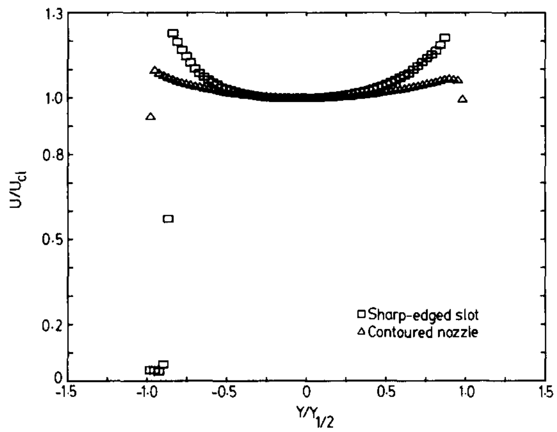

Figure 4 Mean streamwise velocity profiles at the nozzle exit plane

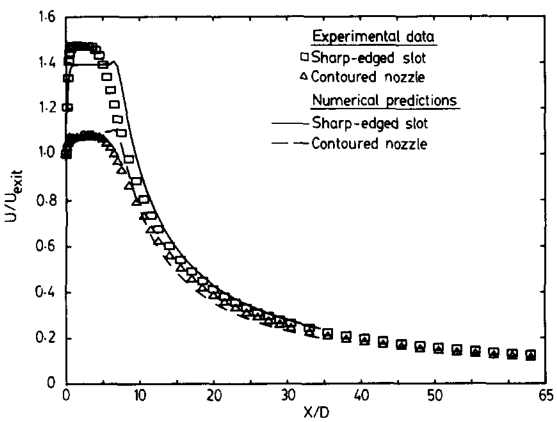

Figure 5 Mean streamwise velocity decay on the jet centerline

changes in mean streamwise velocity that occur within a short distance in the initial region.

Mean streamwise velocity profiles

The mean streamwise velocity off-center peaks, which were present at the nozzle exit plane as a result of streamline curvature (Figure 4), are still distinctly evident downstream in the jet from the sharp-edged slot (Figure 6(a)) but are barely

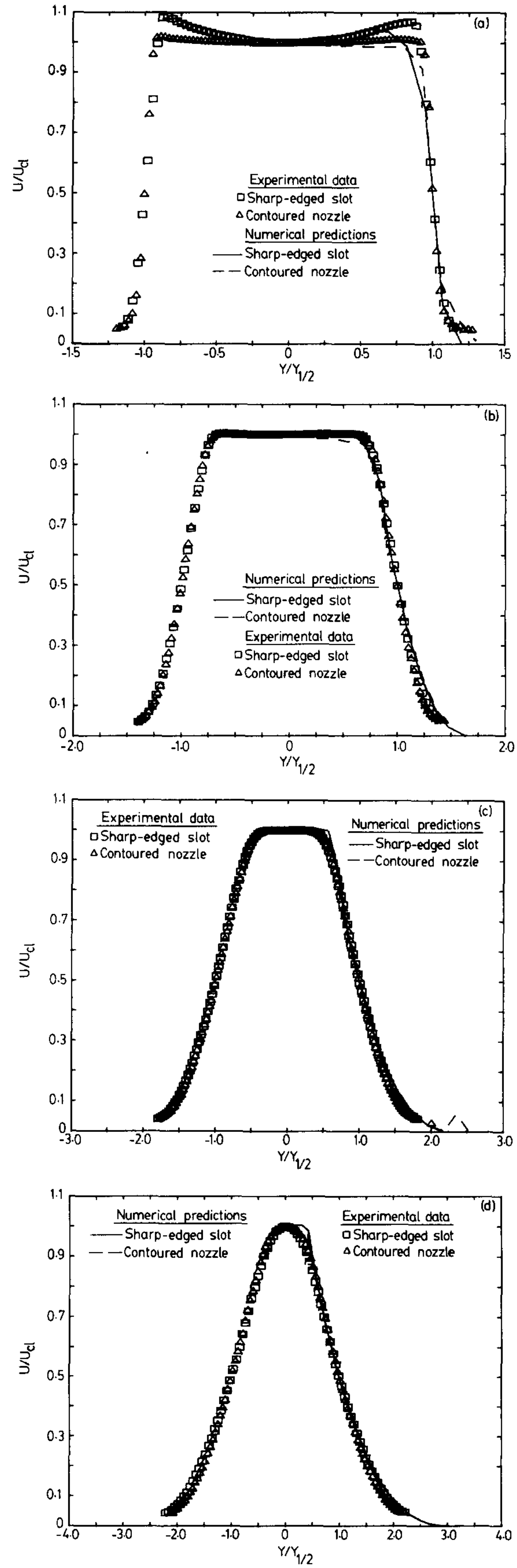

Figure 6 Mean streamwise velocity profiles: (a) $X/D=0.28$; (b) $X/D=1.12$; (c) $X/D=2.66$; (d) $X/D=4.48$

noticeable in the jet from the contoured nozzle which has a significantly lower level of nonparallel exit flow (Figure 4). Further downstream (Figures 6(b), (c), (d)), the mean streamwise velocity profiles for both jets fall on a single curve. Note that the convergence of the flow, brought about by the vena contracta effect, ends at a distance of about half a nozzle diameter downstream of the nozzle exit plane.[24]

The agreement between the experimental and numerical results is good downstream of the location of the vena contracta (Figures 6(b), (c), (d)). The lack of quantitative agreement upstream of the vena contracta is due, as mentioned above, to the coarseness of the grid used.

Spreading

The test jets spread at about the same rate outside the initial region (Figure 7). In the initial region, the jet from the contoured nozzle spreads faster than the jet from the sharp-edged slot. This should be expected because the vena contracta effect, which leads to flow contraction downstream of the nozzle exit plane, is more severe in the jet from the sharp-edged slot than in the jet from the contoured nozzle (Figure 5). The faster spreading of the jet from the contoured nozzle, in the initial region, implies a higher rate of entrainment of ambient fluid.

The nonstandard model constants ($C_{1\varepsilon} = 1.48$ and $C_{2\varepsilon} = 1.90$) helped to ensure a reasonable agreement between the experimental and numerical results for the spreading of the test jets.

Turbulence intensity profiles

The streamwise turbulence intensity profiles (Figures 8(a), (b), (c), and (d)) and the radial turbulence intensity profiles (Figures 9(a), (b), (c), and (d)) show the same general behavior. Low values of the turbulence intensities are found in regions of the flows (e.g., close to the centerline) where the local shear in the mean streamwise velocity is either nonexistent or has a low value. High turbulence intensity values exist in the shear layer regions where there is high local shear in the mean streamwise velocity and the consequent high production of turbulence.

The radial turbulence intensities in the jet from the contoured nozzle are larger than those in the jet from the sharp-edged slot just downstream of the exit plane (Figures 9(a), (b)). This is consistent with the faster spreading of the jet from the contoured nozzle in the initial region (Figure 7).

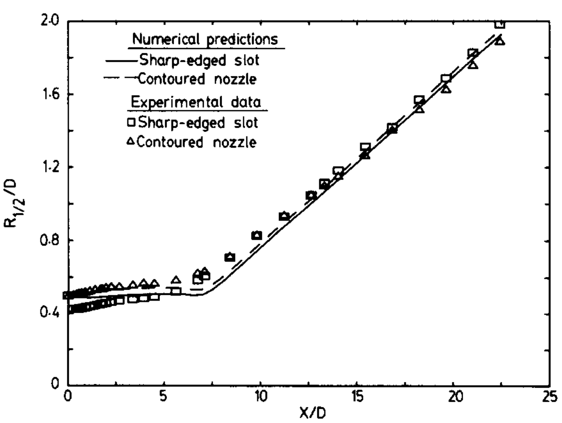

Figure 7 Spreading

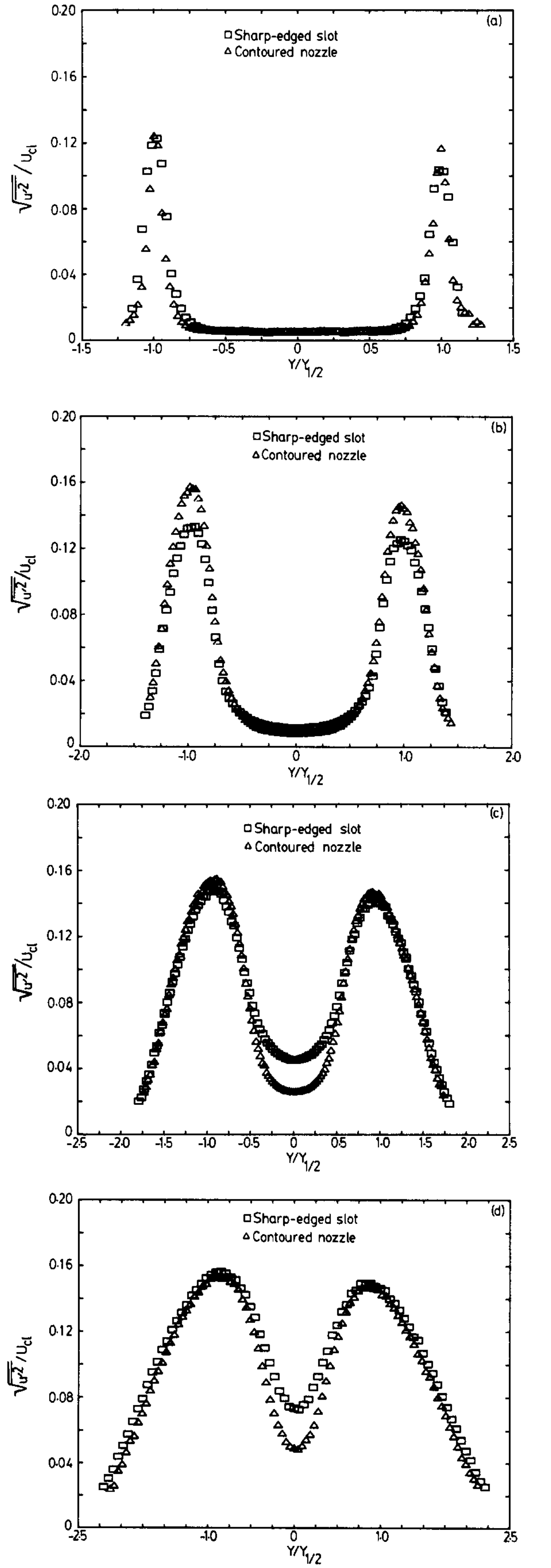

Figure 8 Streamwise turbulence intensity profiles: (a) $X/D = 0.28$; (b) $X/D = 1.12$; (c) $X/D = 2.66$; (d) $X/D = 4.48$

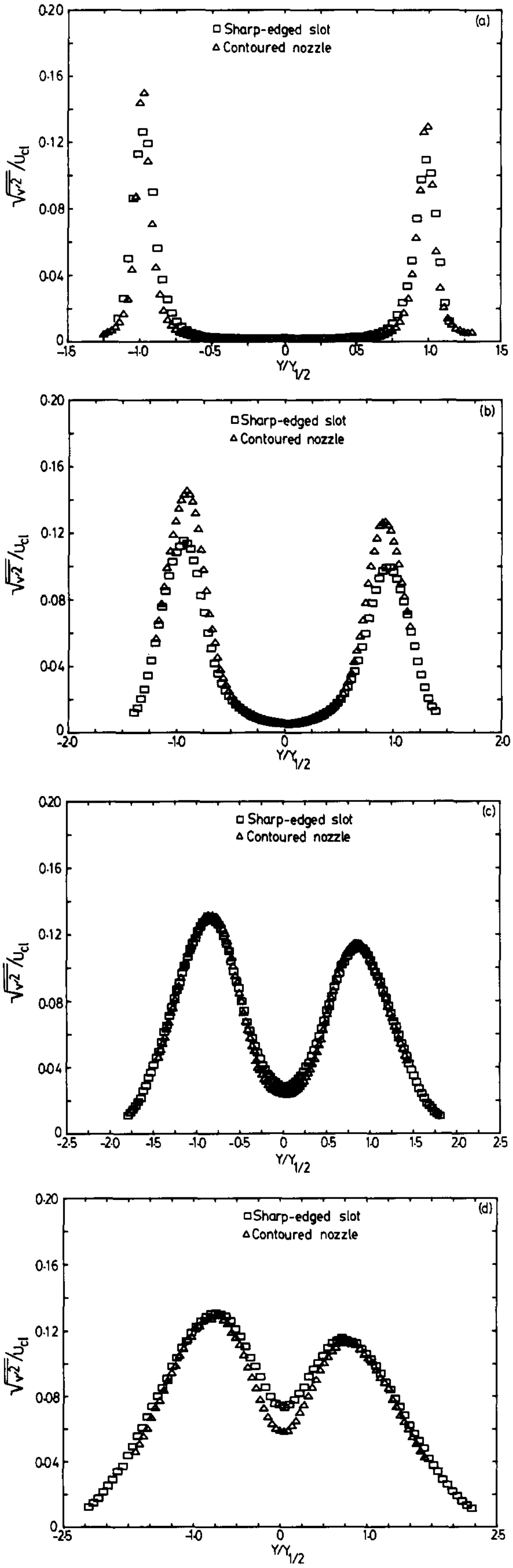

Figure 9 Spanwise turbulence intensity profiles: (a) $X/D = 0.28$; (b) $X/D = 1.12$; (c) $X/D = 2.66$; (d) $X/D = 4.48$

Mean static pressure profiles

The experimental results for the mean static pressure (Figures 10(a), (b), and (c)) reveal positive (i.e., above atmospheric pressure) values in the central regions and, as expected, negative values in the shear layer regions. The boundary layer form of the radial momentum equation can be used to show that negative mean static pressures must exist in the fully turbulent regions of turbulent free jets. Positive mean static pressures, which have also been reported for turbulent plane free jets,[25,26] are only found in the quasi-inviscid cone bounded by the shear layers in free turbulent jets.

The mean static pressure minima (Figures 10(a), (b), and (c)), which are negative, occur where the radial turbulence intensity maxima (Figures 9(a), (b), and (c)) are found. This

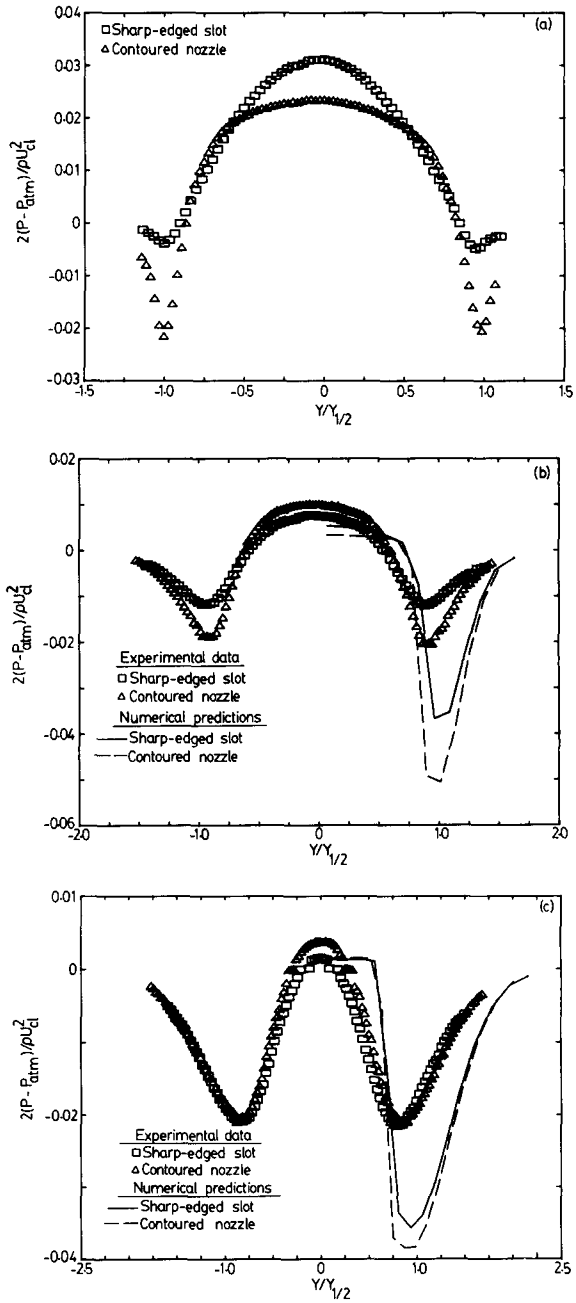

Figure 10 Mean static pressure profiles: (a) $X/D = = 0.28$; (b) $X/D = 1.12$; (c) $X/D = = 2.66$

indicates that the boundary layer form of the radial momentum equation can be applied to the shear layers in the initial region.

The experimental data for the mean static pressure are subject to the uncertain errors due to turbulence.[27] These data which make a useful contribution toward the understanding of the physics of the flow can, therefore, only be regarded as qualitative. It has, however, been shown[28] that pitot-static tubes, of sizes frequently used in experimental work, measure the mean static pressure in turbulent jets with an error less $\pm 2\%$ of the local dynamic head on the jet centerline. This error stems from the mean yaw and pitch angles of the velocity vector. It is interesting to note that the experimental mean static pressure minima (Figures 10(b), (c)) are at most within 3% of the numerically predicted minima.

A possible source of error in the numerical predictions for the mean static pressure is numerical diffusion which is a consequence of the coarseness of the grid used in the initial region. Numerical diffusion coefficients were evaluated, following de Vahl Davis and Mallinson,[29] and the values compared to those of the turbulent diffusion coefficient at the control volume nodes located at streamwise distances of $0.5D$ and $1.0D$ and radial distances of $0.31D$, $0.44D$, and $0.5D$. It was found that the numerical diffusion coefficients were one order of magnitude smaller than the turbulent diffusion coefficients where the Peclet numbers were large $(>10^3)$ and both sets of coefficients were of the same order of magnitude where the Peclet numbers were small (<30). The numerical mean static pressure predictions for the flow from the contoured nozzle should be more accurate than those for the sharp-edged slot flow which has large streamline inclination in the initial region due to the fairly large mean radial velocities.

Conclusions

The effects of nonparallel exit flow on flow in the initial region of round turbulent free jets have been studied experimentally and numerically. Two round nozzles were used: a sharp-edged slot machined into a plate of aluminum and a smoothly contoured nozzle made from Plexiglas.

Distinct mean streamwise velocity off-center peaks were found within half a nozzle diameter downstream of the exit plane of the sharp-edged slot. Such mean streamwise velocity off-center peaks were absent downstream in the contoured nozzle flow which was found to spread faster in the initial region.

Acknowledgments

Financial support of the Natural Sciences and Engineering Research Council of Canada, through grants A5484 and A5451, is gratefully acknowledged.

References

1 Wygnanski, I. and Fiedler, H. Some measurements in the self-preserving jet. *J. Fluid Mech.*, 1969, **38**, 577–612

2 Rodi, W. A new method of analysing hot-wire signals in highly turbulent flow, and its evaluation in a round jet. *DISA Info.*, 1975, **17**, 9–18

3 Rajaratnam, N. *Turbulent Jets*, Elsevier, New York, 1976

4 Schlichting, H. *Boundary-Layer Theory*, 6th ed, McGraw-Hill, New York, 1968

5 Rodi, W. The prediction of free turbulent boundary layers by use of a two-equation model of turbulence. PhD Thesis, University of London, 1972

6 Spalding, D. B. Concentration fluctuations in a round turbulent free jet. *Chem. Engng. Sci.*, 1971, **26**, 95–107

7 Givi, P. and Ramos, J. I. On the calculation of heat and momentum transport in a round jet. *Int. Comm. Heat Mass Transfer*, 1984, **11**, 173–182

8 Davies, P. O. A. L., Fisher, M. J., and Barratt, M. J. The characteristics of turbulence in the mixing region of a round jet. *J. Fluid Mech.*, 1963, **15**, 337–367

9 Bradshaw, P., Ferriss, D. H., and Johnson, R. F. Turbulence in the noise-producing region of a circular jet. *J. Fluid Mech.*, 1964, **19**, 591–624

10 Ko, N. W. M. and Davies, P. O. A. L. The near field within the potential cone of subsonic cold jets. *J. Fluid Mech.*, 1971, **50**, 49–78

11 Lau, J. C. and Fisher, M. J. The vortex-street structure of "turbulent" jets. Part 1. *J. Fluid Mech.*, 1975, **67**, 299–337

12 Crow, S. C. and Champagne, F. H. Orderly structure in jet turbulence. *J. Fluid Mech.*, 1971, **48**, 547–591

13 Dimotakis, P. E., Miake-Lye, R. C., and Papantoniou, D. A. Structure and dynamics of round turbulent jets. *Phys. Fluids*, 1983, **26**, 3185–3191

14 Hussain, A. K. M. F. Coherent structures—reality and myth. *Phys. Fluids*, 1983, **26**, 2816–2850

15 Sami, S., Carmody, T., and Rouse, H. Jet diffusion in the region of flow establishment. *J. Fluid Mech.*, 1967, **27**, 231–252

16 Hill, B. J. Measurement of local entrainment rate in the initial region of axisymmetric turbulent air jets. *J. Fluid Mech.*, 1972, **51**, 773–779

17 Boguslawsi, L. and Popiel, Cz. O. Flow structure of the free round turbulent jet in the initial region. *J. Fluid Mech.*, 1979, **90**, 531–539

18 Obot, N. T., Graska, M. L., and Trabold, T. A. The near field behaviour of round jets at moderate Reynolds numbers. *Canadian J. Chem. Engng.*, 1984, **62**, 587–593

19 Patankar, S. V. *Numerical Heat Transfer and Fluid Flow*, Hemisphere, New York, 1980

20 Spalding, D. B. Mathematical modelling of fluid mechanics, heat transfer and chemical-reaction processes. Imperial College, CFDU Report No. HTS/80/1, 1980

21 Launder, B. E. and Spalding, D. B. The numerical computation of turbulent flows. *Comp. Meths. Appl. Mech. Engng.*, 1974, **3**, 269–289

22 Rodi, W. Turbulence models for environmental problems. In *Prediction Methods for Turbulent Flows*, ed. W. Kollmann, Hemisphere, Washington, D.C., 1980, 259–349

23 Spalding, D. B. A general purpose computer program for multidimensional one- and two-phase flow. *Mathematics and Computers in Simulation*, 1981, **23**, 267–276

24 Daugherty, R. L., Franzini, J. B., and Finnemore, E. J. *Fluid Mechanics with Engineering Applications*, McGraw-Hill, New York, 1985

25 Miller, D. R., and Comings, E. W. Static pressure distribution in the free turbulent jet. *J. Fluid Mech.*, 1957, **3**, 1–16

26 Sunyach, M. and Mathieu, J. Zone de melange d'un jet plan fluctuations induites dans le cone a potentiel-intermittence. *Int. J. Heat Mass Transfer*, 1969, **12**, 1679–1697

27 Hinze, J. O. *Turbulence*, 2nd ed, McGraw-Hill, New York, 1975

28 Bradshaw, P. and Goodman, D. G. The effect of turbulence on static-pressure tubes. Aeronautical Research Council Reports and Memoranda No. 3527, September, 1966

29 de Vahl Davis, G. and Mallinson, G. D. False diffusion in numerical fluid mechanics. School of Mechanical and Industrial Engineering, University of New South Wales Report No. 1972/FMT/1, 1972